Asian Journal of Physics Vol. 24, No 1 (2015) 17-32

On the methods of measurement of radius of curvature and focal length

Rajpal S Sirohi
Department of Physics,Tezpur University, Napaam
Tezpur-784 028, India

Dedicated to Prof G D Baruah

Radius of curvature of spherical surfaces and the focal length of optical imaging systems are very important parameters to be measured. Large number of techniques and methods have been developed over the years. They offer varying accuracy and ranges. However, the complexities of measurement increase depending on the desired accuracy and range. The paper presents a variety of techniques and methods that include contact type and non-contact type methods.

1 Introduction

All optical components are bound by the combination of plane and curved surfaces. The curved surfaces provide power to the element. Due to ease of fabrication, the curved surfaces are spherical, though non-spherical and free form surfaces are gaining importance in some sophisticated designs. The spherical surfaces need to be produced with tight tolerances on the surface curvature. The measurement of radii of curvature of surfaces and focal lengths of lenses and mirrors is a very important activity in the production environment. It is the range, and the accuracy and precision required that make these measurements often very complicated. In most of the cases, the measurement procedure is straightforward. But the complexities abound when the measurement involves extremes in the range; the range may span from a millimeter to several meters. The paper discusses the principles of various methods and procedures used for measuring these parameters.

2 Measurement of radius of curvature

Both the mechanical and the optical means are used to measure the radii of curvature of the surfaces [1-5]. Each of these methods can be grouped into two categories: (i) indirect method in which either the sagitta or the slope of the surface is measured, and (ii) direct method in which distance between the positions of the vertex and the center of curvature is measured. It should be noted that the surfaces are assumed to be part of a sphere. The methods under this category do not measure the departure from sphericity but yield an average radius of curvature of a surface.

A-1 Indirect Method: Measurement of Sagitta

Sagitta can be measured either using a mechanical spherometer or an optical spherometer. It can also be measured interferometrically such as in Newton's ring method.

A-1.1 Mechanical Spherometer

Usually a mechanical spherometer is a three-leg instrument: the three pointed legs being at the vertices of an equilateral triangle [4]. A central plunger is used to measure the sagitta. The instrument is adjusted by placing it on a plane surface, contacting the surface with the plunger and taking the readings. These readings act as a reference. The instrument is then placed on a spherical surface and the readings are taken when the plunger touches the surface. The difference between these two readings is the sagitta. It can be shown that the radius of curvature R is related to the measured sagitta h as

$$R = \frac{a^2}{6h} + \frac{h}{2} \tag{1}$$

Corresponding author :
e-mail: rs_sirohi@yahoo.co.in (Rajpal S Sirohi)

where a is the length of the arm of an equilateral triangle. Often the pointed legs are replaced by the legs carrying balls of radii r. In this case a small correction is made to the measured sagitta and the radius of curvature is now given by

$$R = \frac{a^2}{6h} + \frac{h}{2} \pm r \tag{2}$$

where + sign is used for concave surface and – is used for the convex surface. The expression (2) is easily obtained following the Fig (1a) as

$$(R - r)^2 = d^2 + [R - (h + r)]^2 \quad \rightarrow \quad R = \frac{d^2}{2h} + \frac{h}{2} + r \tag{3}$$

But the value of d in terms of the length a of the arm of the equilateral triangle (Fig 1b) is obtained as

$$\frac{a}{2} = d \cos 30° = d\,\frac{\sqrt{3}}{2} \quad \rightarrow \quad d = \frac{a}{\sqrt{3}} \tag{4}$$

Substituting for d in Eq (3), we obtain

$$R = \frac{a^2}{6h} + \frac{h}{2} + r \tag{5}$$

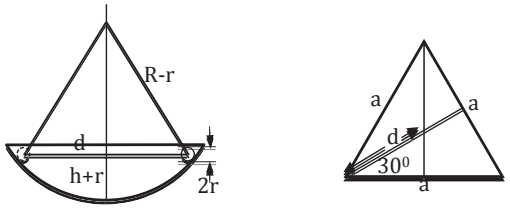

(a) (b)

Fig 1. (a) Determination of sagitta, (b) relation between a and d

When the spherometer with a ring base is used, the radius of curvature is given by

$$R = \frac{y^2}{2h} + \frac{h}{2} \tag{6}$$

where y is the radius of the ring. The ring has sharp edge, which contacts with the spherical surface and may scratch it. Instead of the ring, one can have three balls of radius r mounted on it. In that case, the radius of curvature is given by

$$R = \frac{y^2}{2h} + \frac{h}{2} \pm r \tag{7}$$

Same formula (Eq 7) applies when a ring of circular section of radius r is used in place of three balls.

Assuming that y and r are accurately known, the uncertainty ΔR in R due to the uncertainty Δh in the measurement of the sagitta h can be expressed as

$$\Delta R = \frac{\Delta h}{2}\left(1 + \frac{y^2}{h^2}\right) \tag{8}$$

where the uncertainties have been added.

A bar spherometer is used for the evaluation of astigmatism. It is in the shape of a bar with the contact points at the ends and spindle at the center for measurement. It can measure the curvature along any diameter [6]. The Geneva gauge is a commercial version of the bar spherometer for optometric work. Its scale is directly calibrated in diopters assuming that the refractive index of the glass is 1.523.

Methods based on physical contact require an application of constant pressure for each measurement. It is implied that the pressure must not deform the surface. Therefore, non-contact methods are preferred against the contact methods.

A-2 Direct Methods

A-2.1 Image formation

Concave mirror forms an image of an object with unit magnification when the object is placed at the center of curvature, i.e. the image is formed where the object is, as shown in Fig 2. Then the distance between the object plane and the vertex of the mirror is the radius of curvature.

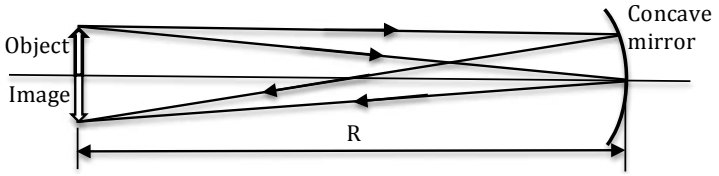

Fig 2. Measurement of radius of curvature of a concave spherical mirror

A-2.2 Differences in conjugate positions

There could be a significant error in locating the vertex of the mirror, and hence the distances of the object and image could also be in error resulting in a significantly large error in the value of the measured curvature. However, if we could locate a reference point with respect to which the distances are measured, more accurate value of the radius of curvature can be obtained. For this purpose, center of curvature is taken as the reference point, which is located by making an image of a point object on itself as shown in Fig 3. We can now place an object at any position O_1 and obtain its image by sliding a small screen (or a detector) from the plane passing through the center of curvature. Let this position be I_1. The point object is now moved to a different location O_2 and its image is obtained at I_2. Let the distances between the center of curvature C and I_1 be b and between C and I_2 be c. Further the separation between the object positions O_2 and O_1 be a. These distances can be measured accurately as these are the differences between the two positions.

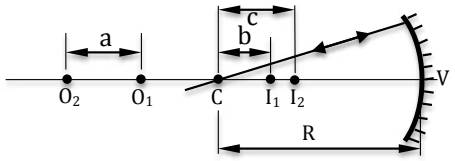

Fig 3. Imaging in a spherical concave mirror

Using imaging conditions, we have

$$\frac{1}{p} + \frac{1}{R-b} = \frac{2}{R} \tag{9a}$$

and

$$\frac{1}{p+a} + \frac{1}{R-c} = \frac{2}{R} \tag{9b}$$

where p is the distance of object point at O_1 as measured from the vertex V and is unknown and R is the distance between vertex V and center of curvature C, which is to be determined.

Eliminating p and rearranging, we obtain

$$R^2 (a + b - c) - 2Ra(b + c) + 4abc = 0 \tag{10}$$

The solution of the quadratic equation (10) gives the value of R as

$$R = \frac{a(a+b) + \sqrt{a^2(b+c)^2 - 4abc\,(a+b-c)}}{(a+b-c)} \tag{11}$$

By inserting the numerical values of a, b and c, the radius of curvature R is calculated. Note a, b and c are the difference values and known to an accuracy of the least count of the optical bench on which the experiment is conducted.

A-2.3 Optical Spherometer

A point focus microscope along with a suitable measuring rail constitutes the optical spherometer [7-15]. The microscope and the test surface are mounted on the rail. For a concave surface, two positions can be found which give the point image on retro-reflection. The separation between these positions is the radius of curvature of the surface. For making measurement on the convex surface, additional lens is required which must have its focal length larger than the radius of curvature of the surface being measured. Figure 4 shows the experimental arrangements.

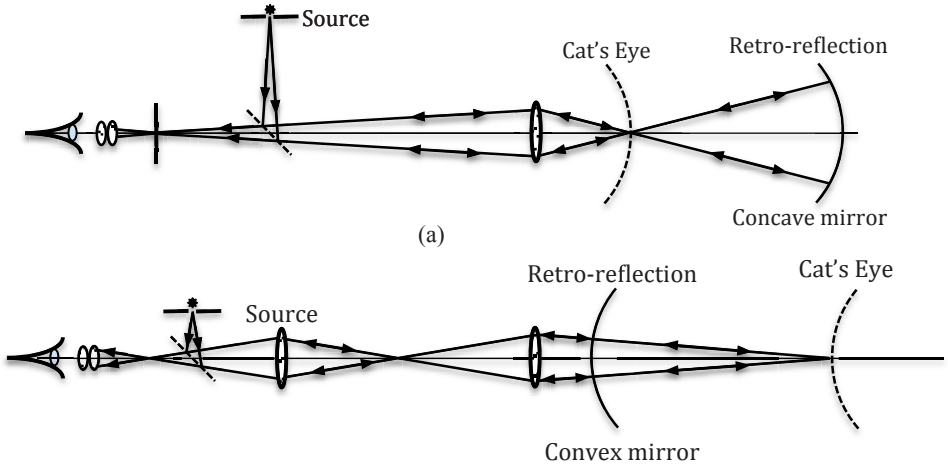

Fig 4. Determination of radius of curvature of (a) concave, (b) convex spherical surface

For moderate range (~ 1m to 2m) an autocollimator with a suitable lens can also be used to obtain cat's eye and confocal positions. A Twyman-Green or a Fizeau interferometer can also be used to determine these locations by observing null in the interference pattern. A long coherence length laser is used as a source. With careful implementation, the radius of curvature of the spherical surfaces can be measured to an accuracy of a few parts in 10^5.

A-3 Measurement of long radius of curvature

A-3.1 Newton's Rings Method

For the measurement of very long radii of curvature of the spherical surfaces, the methods employing measurement of sagitta by mechanical means or the direct distance measurement are not suitable: - the first due to the accuracy of measurement of the sagitta and the second due to the availability of space and optics considerations.

However, sagitta can be measured interferometrically with good accuracy [16]. For measuring long radii of curvature, interference methods such as Newton's ring method along with phase shifting could be used. The radius of curvature R and radius ρ_m of the m^{th} circular fringe in the Newton's rings pattern is related by

$$\rho_m = \sqrt{m\lambda R} \quad \text{or} \quad R = \frac{\rho_m^2}{m\lambda} \tag{12}$$

Value of the radius of curvature is obtained from the slope of ρ_m^2 vs. m plot. The Talbot effect has also been utilized to measure moderate to long radii of curvature of the spherical surfaces.

A-3.2 Cavity Method

Gerchman and Hunter presented a method in which a cavity is formed between the concave surface under test and a plane surface [17]. A parallel (collimated) beam is incident on the concave surface, which focuses it at a point where a plane surface is placed, which retro-reflects the beam. In fact many such positions can be found by changing the separation between the plane surface and the concave surface such that the beam is focused on either of the two surfaces resulting in retro-reflection. This greatly reduces the working space required for measurement.

When a collimated beam is incident on the concave surface, it is brought to a point focus at a distance $R/2$, where the plane surface is placed. This arrangement is called $n = 1$ configuration. When the plane surface is moved towards the concave surface such that the beam is focused on the concave surface, this results in $n = 2$ configuration. Further shift of the plane mirror results in focusing of the beam at the plane surface which is $n = 3$ configuration. The process can continue for higher order configurations. When n is odd, the focus is on the plane surface and for n even it is on the concave surface. The separation between two successive such positions is used to obtain the value of the radius of curvature.

Let z_n be the separation between the concave and the plane surfaces (cavity length) for the n^{th} configuration. The equations that relate the cavity length z_n and the radius of curvature R of the concave surface are derived from paraxial ray analysis. This is accomplished by repeated application of the Gaussian image equation given by

$$\frac{1}{p_m} + \frac{1}{q_m} = \frac{2}{R} \tag{13}$$

and the conjugate recursion formula

$$p_m = 2z_n - q_{m-1} \tag{14}$$

where $m = k, k-1, k-2, \ldots\ldots, 0$, and $k = (n-1)/2$ for odd n and $k = (n-2)/2$ for even n.

An appropriate initial condition is determined for each configuration depending upon where the system comes to focus. These initial conditions are: for n odd, $z_n = q_k$ and for n even, $z_n = q_k/2$.

We will now apply these equations to obtain the cavity length for 7^{th} order configuration. Therefore, $n = 7$, and $k = 3$. This gives m values as 3, 2, 1 and 0. Further we have the following equations

$$p_3 = 2z_7 - q_2 \tag{15a}$$

$$p_2 = 2z_7 - q_1 \tag{15b}$$

$$p_1 = 2z_7 - q_0 \tag{15c}$$

$$z_7 = q_2 \tag{15d}$$

Figure 5 shows the geometry of 7^{th} order cavity with the ray paths showing the positions p_m and q_m. Using the Gaussian imaging relation $\frac{1}{p_3} + \frac{1}{q_3} = \frac{2}{R}$, and substituting for q_3, we solve it for p_3 as

$$p_3 = \frac{R\, z_7}{2z_7 - R} \tag{16}$$

Using Eq (15a), we obtain

$$p_3 = \frac{R\, z_7}{2z_7 - R} = 2z_7 - q_2 \quad \Rightarrow \quad q_2 = \frac{4z_7^2 - 3R\, z_7}{2z_7 - R} \tag{17}$$

We now apply the Gaussian imaging condition for $m = 2$, i.e.

$$\frac{1}{p_2}+\frac{1}{q_2}=\frac{2}{R} \;\Rightarrow\; \frac{1}{p_2}=\frac{2}{R}-\frac{2z_7-R}{4z_7^2-3R\,z_7} \;\Rightarrow\; p_2=\frac{4R\,z_7^2-3R^2\,z_7}{8z_7^2-8R\,z_7+R^2} \tag{18}$$

Using Eq (15b), we have

$$p_2=\frac{4R\,z_7^2-3R^2\,z_7}{8z_7^2-8R\,z_7+R^2}=2z_7-q_1 \;\Rightarrow\; q_1=\frac{16\,z_7^2-20R\,z_7^2+5R^2z_7}{8\,z_7^2-8R\,z_7+R^2} \tag{19}$$

Now applying Gaussian imaging condition for $m = 1$, we have

$$\frac{1}{p_1}+\frac{1}{q_1}=\frac{2}{R} \;\Rightarrow\; \frac{1}{p_1}=\frac{2}{R}-\frac{8\,z_7^2-8R\,z_7+R^2}{16\,z_7^3-20R\,z_7^2+5R^2z_7} \tag{20}$$

This gives

$$p_1=\frac{16R\,z_7^3-20R\,z_7^2+5R^{\,3}z_7}{32\,z_7^3-48\,R\,z_7^2+18R^3z_7-R^3} \tag{21}$$

Using Eq (15c), we have

$$p_1=\frac{16R\,z_7^3-20R\,z_7^2+5R^{\,3}z_7}{32\,z_7^3-48\,R\,z_7^2+18R^3z_7-R^3}=2z_7-q_0$$

$$\Rightarrow\; q_0=\frac{6R\,z_7^4-112R\,z_7^3+56R^2z_7^2+7R^3z_7}{32\,z_7^3-48\,R\,z_7^2+18R^3z_7-R^3} \tag{22}$$

Now applying Gaussian imaging condition for $m = 0$, we have

$$\frac{1}{p_0}+\frac{1}{q_0}=\frac{2}{R} \;\Rightarrow\; \frac{1}{p_0}=\frac{2}{R}-\frac{32\,z_7^3-48\,R\,z_7^2+18R^3z_7-R^3}{64\,z_7^4-112\,R\,z_7^3+56\,R^2z_7^2+7R^3z_7} \tag{23}$$

This gives

$$p_0=\frac{64R\,z_7^4-112R^2z_7^3+56R^3z_7^2+7R^4z_7}{128\,z_7^4-256\,R\,z_7^3+160\,R^2z_7^2-32\,R^3z_7+R^4} \tag{24}$$

Table 1

	Cavity length z_n	**Radius vs differential cavity length**
n	z_n	
1	0.5 R	$R = 4\,(z_1 - z_2)$
2	0.25 R	$R = 9.65685\,(z_2 - z_3)$
3	0.1464466 R	$R = 19.62512\,(z_3 - z_4)$
4	0.0954915 R	$R = 35.08255\,(z_4 - z_5)$
5	0.0669873 R	$R = 57.23525\,(z_5 - z_6)$
6	0.0495156 R	$R = 87.29584\,(z_6 - z_7)$
7	0.0380603 R	$R = 126.47741\,(z_7 - z_8)$
8	0.0301537 R	$R = 175.99437\,(z_8 - z_9)$
9	0.0244717 R	

Since collimated beam is incident on the concave surface, $p_0 = \infty$. Therefore

$$128\,z_7^4-256\,R\,z_7^3+160\,R^2z_7^2-32\,R^3z_7+R^4=0 \tag{25}$$

The solution of this equation is $z_7 = 0.0380603R$. Essentially one can solve for the cavity length for any value of n. The values for z_3, z_4, z_5 and z_6 are: $z_3 = 0.1464466R$, $z_4 = 0.0954915R$, $z_5 = 0.0669873R$ and $z_6 = 0.0495156R$. Thus the cavity length z_n is related with the radius of curvature R of the concave surface through a relation $z_n = C_n R$, where the values of C_n for first 9 configurations are given in Table 1. This table also gives the relationships between the radius of curvature and differential cavity length ($z_n - z_{n-1}$).

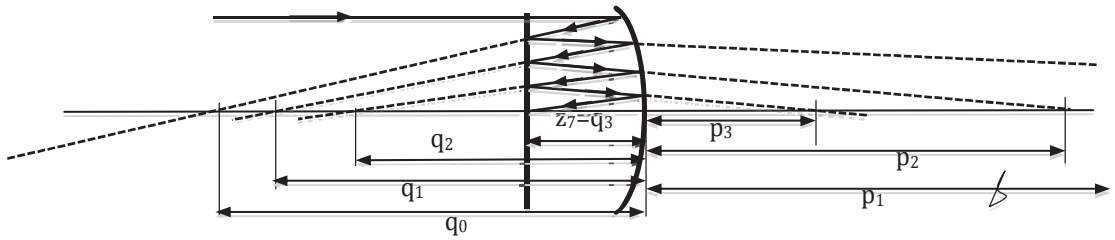

Fig 5. Ray path for 7 reflections cavity method

A-4 Measurement of very long radii of curvature

A-4.1 Interferometric Methods

Sagitta of a concave or a convex surface can also be measured interferometrically [16]. A flat surface is placed on the spherical surface. It makes a contact at the center when the spherical surface is convex creating a thin film of air. For the concave surface, the contact is at the edge of the flat or edge of the concave surface whichever is smaller. A collimated beam illuminates this arrangement and the interference takes place between the beams reflected from the top and the bottom of the air film as shown in Fig 6. The fringes are fringes of constant thickness and hence are circular in form. The order of fringe is zero at the center for a convex spherical surface and increases outwardly. The center fringe is black due to phase change of π at the air-glass interface. For a concave surface, the order is zero at the contact circle and increases towards the center.

(a) (b)

Fig 6. Interference in a thin film between a flat surface (a) convex surface (b) concave surface

Consider a convex surface on top of which is placed a flat surface. It can be shown that the radius r_n of the n^{th} dark ring due to interference between plane and convex surface is given by

$$r_n = \sqrt{n\lambda R} \tag{26}$$

where R is the radius of curvature of the convex surface. This is valid when the radius of curvature is very large. This equation can be modified to yield radius of curvature of the convex surface as

$$R = \frac{D^2_n - D^2_{n-1}}{4\lambda} \tag{27}$$

where D_n and D_{n-1} are the diameters of n^{th} and $(n-1)^{th}$ fringes. It is to be seen that the center point $n = 0$

is dark. The diameters of rings can be measured using a travelling microscope. A graph D_n^2 vs n will be linear and its slope is $4\lambda R$.

From the Eq (26) it is to be noted that [16]

$$1 + \frac{D^2_{n+1} - D^2_n}{D^2_{n+2} - D^2_{n+1}} \approx 1 + \frac{1}{2n} \tag{28}$$

The fringe width, for large value of n is practically constant.

For a concave surface, the shape of the air-film is as shown in the Fig (6b). The flat surface makes a contact at the periphery. The film thickness t_0 is a maximum at the center. Let $t(y)$ be the thickness at a location y from the center. Therefore, $y^2 = (2R - t_y)t_y$

where $t_y = t_0 - t(y)$. Under the condition R >> t_0, we have

$$2[t_0 - t(y)] = \frac{y^2}{R} = m'\lambda = (m_0 - m)\lambda \tag{29}$$

where m_0 is the fringe order corresponding to the thickness t_0, which necessarily is not an integer and is not known and m is the fringe order at location y. The fringe order is zero at the point of contact. Due to circular symmetry, the fringes are circular. From this equation we have

$$D^2_{m_0 - m} = 4R\,(m_0 - m)\lambda \tag{30a}$$

$$D^2_{m_0 - m - 1} = 4R\,(m_0 - m - 1)\lambda \tag{30b}$$

On subtraction, we obtain

$$D^2_{m_0 - m} - D^2_{m_0 - m - 1} = 4R\,\lambda \tag{31}$$

This is the same formula (Eq 27) that was obtained for the convex surface. The radius of the concave surface is obtained from the slope of $D^2_{m_0 - m}$ vs $(m_0 - m)$ plot.

The method works fine when there are several circular fringes in the interference pattern; the circular shape of fringes implies that the surface is spherical. However, when the radius of curvature is large, there are a fewer fringes, but the method can still be applied. However, when the number of fringes becomes less than one, the method breaks down. In such a situation, the center of fringe pattern is shifted by lightly tilting the test piece. The fringes now are the arcs of circles. These arcs of circles are nearly equidistant. Let us assume that n^{th} fringe passes through the middle of the test surface as shown in the Fig 7.

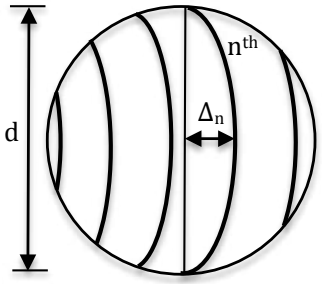

Fig 7. Interferometric measurement of large radius of curvature

Therefore,

$$D^2_{n+1} - D^2_n = (D_{n+1} - D_n)\,(D_{n+1} + D_n) = 4R\,\lambda \tag{32}$$

and

$$\Delta_n D_n = \frac{d^2}{4} \tag{33}$$

In Eq (29), the difference $(D_{n+1} - D_n)$ is two times the fringe width, $\bar{x}$, and $D_{n+1} \approx D_n$, and hence

we have

$$\frac{\Delta_n}{\bar{x}} = \varepsilon = \frac{d^2}{4\lambda R} \Rightarrow \; R = \frac{d^2}{4\lambda\varepsilon} \tag{34}$$

The radius of curvature is obtained by measuring the sag Δ_n and fringe width. It is to be noted that Newton's ring method can be applied to measure short to very large radii of curvature.

A-4.2 Radius of curvature with a test plate

Test plates are made by grinding and polishing two identical circular plates [16]. The process generates a spherical surface, whose radius of curvature can be measured by some other independent procedure. The process of grinding and polishing is continued till the required radius of curvature is achieved. Either of them is called a test plate, which is used to check the radius of curvature of the component being fabricated in the production shop. Convex test plate is used to check a concave surface and vice versa.

If the radius of curvature of the test surface is different than that of the test plate, circular fringes are observed. One can also determine whether the radius of curvature of test surface is smaller or larger than that of the test plate. Let the radius of curvature of the test plate be R, and that of the test surface be $R+\Delta R$. Further let the diameter of the test plate be d. It can be shown that the gap perpendicular to one of the surfaces at a distance r_n from the point of contact is given by

$$\Delta_n = \Delta R\,(1 - \cos\theta) \tag{35}$$

where θ is given by $\sin\theta = \frac{r_n}{R}$, where r_n is the radius of the n^{th} circular fringe. Fringe of n^{th} order will be formed when $2\Delta_n = n\lambda$. Substituting for Δ_n and with little manipulation, we obtain

$$r_n^{\,2} = n\lambda\,\frac{R^2}{\Delta R} \Rightarrow \; D^2_{\,n} = 4n\lambda\,\frac{R^2}{\Delta R} \tag{36}$$

where D_n is the diameter of the n^{th} fringe. In practice, instead of several circular fringes, one would like to have the radius of curvature of test surface as close to that of the test plate as possible and hence less than one fringe. It is under this condition, one is required to determine the departure from the expected radius of curvature. Therefore, the center of the fringe pattern is shifted by slightly tilting the test surface. The fringes now are the arcs of circles and their sag is used to determine the value of ΔR. As before (Eqs 32 & 33) we set up the following two equations

$$D^2_{\,n+1} - D^2_{\,n} = (D_{n+1} - D_n)\,(D_{n+1} + D_n) = 4\lambda\,\frac{R^2}{\Delta R} \tag{37}$$

and

$$\Delta_n D_n = \frac{d^2}{4} \tag{38}$$

Using these two equations, we obtain

$$\frac{\Delta_n}{\bar{x}} = \varepsilon = \frac{d^2\,\Delta R}{4\lambda R^2} \Rightarrow \; \Delta R = \frac{4\lambda\varepsilon R^2}{d^2} \tag{39}$$

This equation gives the departure of the radius of curvature of test surface from the expected value R.

A-5 Newton's Method

When the distances of an object and its image are measured from the foci, we obtain a formula, which is termed as Newton's lens equation or simply Newton's formula [1-3]. Mathematically

$$z\,z' = f\,f' \tag{40}$$

where z and z' are the extra focal object and image distances, respectively and measured from the front and back focal points. The Eq (40) has been very cleverly used to measure long radius of curvature. Figure 8 shows the schematic of the measurement principle. In the Figure 8, a point object O is imaged at O′ and a convex surface is inserted such that its vertex coincides with the back focus point F′. In this case, $z' = R$ and the focal lengths f and f' are equal. Thus $z = f^2/R$ is the working formula. If z could be measured, then the radius of curvature is obtained from the single measurement.

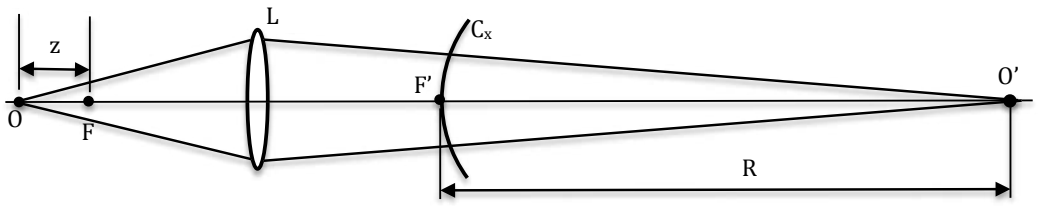

Fig 8. Schematic to measure radius of curvature using Newton's lens equation

The basic question is to how to place the surface exactly at the back focus and measure z accurately. To locate the points O, F and F′, a Fizeau interferometer is utilized and the distance z is measured on a precision linear scale. The procedure is explained in the next paragraph with the help of Fig 9.

Laser beam is expanded and then collimated with lens L_c. The plate P is a partially coated plate, which provides a reference beam. The procedure to locate point F′, F and O, in that order, is as follows:

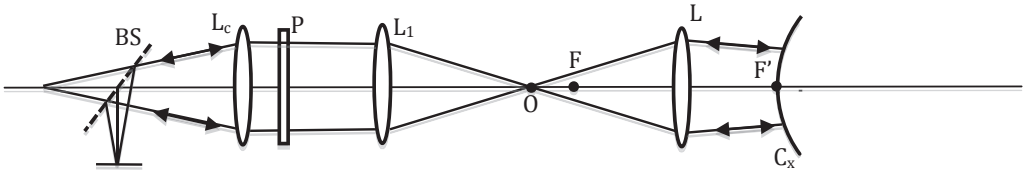

Fig 9. Experimental arrangement to locate points O and F

Lens L is placed in the collimated beam, which focuses the beam to a diffraction focus. The convex surface is now placed in the convergent beam. When properly placed, the beam is retro-reflected (cat's eye position) and a null is obtained between the interference of the reference and retro-reflected beams.

Now the lens L_1 is placed in the beam and a plane mirror is inserted between L and C_x without disturbing the positions of lens L and convex surface C_x. The lens L_1 is translated until the beam existing from lens L is collimated. This position is obtained when the beam reflected from the plane mirror, on interference, gives the null. In this case the back focal point of lens L_1 and front focal point of lens L coincide. Thus the position F is found and the location of L_1 is noted. The plane mirror is removed and the lens L_1 is translated away until the null is obtained. In this case, the rays from lens L strike the surface C_x normally and are retro-reflected (confocal position). This position of lens L_1 is noted and the difference between these two positions is the distance z that is required to determine R. The relative error in the measurement of radius of curvature is given by

$$\frac{\Delta R}{R} = \sqrt{4\left(\frac{\Delta f}{f}\right)^2 + \left(\frac{\Delta z}{z}\right)^2} = \sqrt{4\left(\frac{\Delta f}{f}\right)^2 + \left(\frac{R}{f^2}\right)^2 (\Delta z)^2} \tag{41}$$

where Δf is the accuracy in the measurement of focal length of lens L and Δz is the accuracy in the measurement of distance z.

A-6 Scanning Profilometry

The surface profile can be obtained by measuring the slope along a diameter of the symmetric surface [13, 18]. Let the surface be defined by $z = f(x)$ along the diameter and let $f(0) = 0$. The slope is

measured at locations x_k, the consecutive positions are separated by Δx. Thus $f(x_{k+1}) = f(x_k) + \frac{\Delta x}{2}[f'(x_k) + f'(x_{k+1})]$. Thus integrating the slope values can generate the profile of surface. The radius of curvature is obtained from

$$R = \frac{f''(x)}{\{1+[f'(x)]^2\}^{3/2}} \tag{42}$$

The slope can be measured by an autocollimator in conjunction with a penta-prism, which scans the surface. Higher accuracy is obtained when an interferometric arrangement say when a phase measuring interferometer is used.

A-7 Radius of curvature measurement by Talbot Interferometry

It has been shown that a periodic structure repeats itself when illuminated by a coherent beam. We can make use of this phenomenon to determine the radius of curvature of a spherical surface [19]. Figure [10] shows the schematic of the experimental setup where only the confocal part is shown.

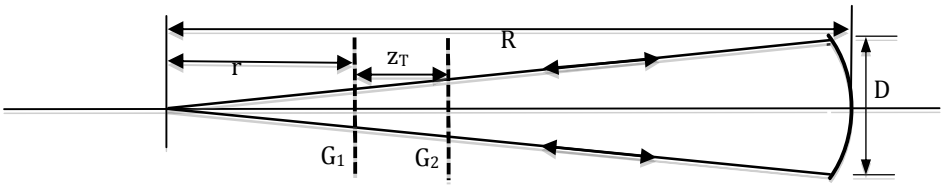

Fig 10. Measurement of radius of curvature by Talbot phenomenon

The grating G_1 of pitch p is illuminated by a diverging wave of radius of curvature r. The Talbot planes are formed at distances z_T, where $z_T = \frac{2N p^2 r}{\lambda r - 2Np^2}$, where N = 1, 2, 3,..for different Talbot planes. The spacing between the successive Talbot planes increases with the order N. The pitch of the grating also increases as if it is geometrically projected, i.e. $p' = p\frac{r + z_T}{r}$. If grating G_2 is placed at the first Talbot plane, moiré pattern due to pitch mismatch is formed. The pitch of the moiré fringe pattern is $p_m = \frac{\Delta r}{2p} - p \approx \frac{\Delta r}{2p}$. The radius of curvature of the wave at the plane of G_1 grating is thus obtained. This could be related to the radius of curvature of the mirror.

Assuming that the illuminated sizes of grating G_1 and G_2 are y and y_1, then

$$p' = p\frac{y_1}{y} = p\frac{y + az_T}{y} = p\left(1 + \frac{az_T}{y}\right) \tag{43}$$

where $a = D/R$. The pitch of the moiré fringe is $p_m = \frac{p\,p'}{p' - p} = \frac{p'y}{a\,z_T}$. If there are n moiré fringes in the pattern formed, then

$$n = \frac{y}{p_m} = \frac{az_T}{p'} = \frac{Dz_T}{Rp'} \Rightarrow R = \frac{Dz_T}{np'} \tag{44}$$

The radius of curvature can be obtained by measuring D, z_T, and noting the number of moiré fringes formed. Often Talbot phenomenon is used for setting purposes.

B-Measurement of Focal Length

B-1.1 Focal length of a thin lens

For a single thin lens, the effective focal lengths f and f' are defined as the distances from the lens vertex to the front focal point and the rear focal point respectively. However, for a thick lens or a lens combination, the effective focal lengths f and f' are the distances between the front focal point and the front

principal point, and the rear principal point and the rear focal point. The back focal length is the distance between the rear vertex to the rear focal point and the front focal length is the distance between the front focal point and the front vertex of the lens. It is easier to measure the back and the front focal lengths.

B-1.2 Focal length by imaging

The simplest though not an accurate method to determine the focal length of a lens is to image a distant object. Since the object is far away, the distance between the lens and the image is the focal length. One could use sun as an object and make its image. Alternately an incandescent or a fluorescent lamp far away in the room could be taken as the luminous object. Using this method focal length can be assigned to within a few millimeters.

A simple arrangement to measure the focal length of a thin positive lens is to use a mesh (gauge) illuminated by a diffuse light source [1-3]. The mesh is placed flushed on a screen that is located on the optical bench. The test lens and a plane mirror behind it are also placed on the bench and their heights are properly adjusted. The lens is moved towards or away from the mesh until its sharp image is formed on the screen. The light retro-reflected by the plane mirror forms this image. The mirror may be tipped a little so that the image is formed along side of the mesh. The distance between the screen and the vertex of the lens is the focal length of the lens.

*B-1.3 y'/*tan θ' *method*

Figure 11 shows an off-axis collimated beam incident on the lens. The image is formed at its focal plane.

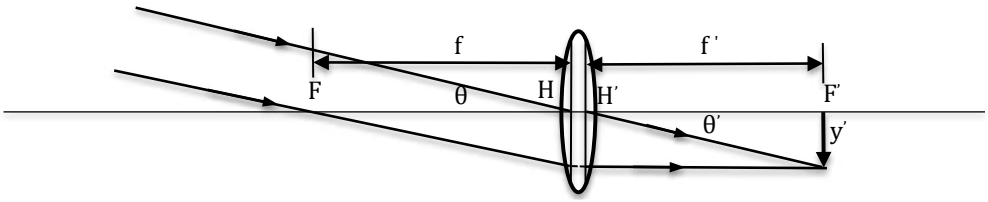

Fig 11. Ray path to measure focal length of a lens

From the Fig 11, $y' = -f \tan\theta = f' \tan\theta'$. When the lens is in air, its nodal planes are coincident with the principal planes and hence its focal lengths f and f' are equal, and the angle θ' in image space is equal to the angle of incidence θ. In practice, $y'/\tan\theta'$ method is implemented by placing a reticle at the focal plane of a collimator. The graduations and the focal length of the collimator are accurately known, implying that the angular size of the object is accurately known. The test lens is placed coaxially with the collimator; the reticle appears at infinity to the test lens and a microscope measures its image formed at the focal plane of the lens. If the measurement is done directly using a translation stage on which the microscope is mounted, the focal length is obtained as

$$f = \frac{y'}{\tan\theta} = \frac{y'}{y_0} f_e \tag{45}$$

where y_0 is the size of the reticle whose image is y' and f_c is the focal length of the collimator. If the graticule in the eyepiece of the microscope is used for measuring, then the measured value of y' is to be divided by the magnification m of the microscope.

B-1.4 Magnification method

Using the lens imaging formula, the lateral magnification M when the media on both sides of the lens are same, can be expressed as

$$M = -\frac{q}{p} = 1 - \frac{q}{f} \tag{46}$$

Further if the distance between object plane and the image plane is more than 4*f*, an image can be formed for several positions of the lens. Therefore, keeping the object and image planes fixed, the test lens is translated to form an image. Let the distance between the vertex of the lens and the object plane be q_i and the corresponding magnification of the image is M_i. The slope of a plot between q_i and M_i gives the inverse of the focal length.

Alternately, the lens can be kept fixed and the object position is varied and the magnification measured at the corresponding image position. Let q_1 and q_2 be the image positions at which the measured magnifications are M_1 and M_2 , respectively. Then

$$M_1 = 1 - \frac{q_1}{f},\ M_2 = 1 - \frac{q_2}{f} \ \Rightarrow (M_2 - M_1) = \frac{|q_2 - q_1|}{f} \tag{47}$$

The separation $(q_2 - q_1)$ can be measured accurately. The method does not require the knowledge of the location of the principal planes.

A variant of this method involves the measurement of the displacement of the object. Let M_1 and M_2 be the magnifications for object positions p_1 and p_2, respectively. Mathematically

$$1 + \frac{1}{M_1} = \frac{p_1}{f} \text{ and } 1 + \frac{1}{M_2} = \frac{p_2}{f} \tag{48}$$

This gives, $f = \dfrac{(p_2 - p_1)\, M_1 M_2}{M_1 - M_2}$. The method is due to Abbe [2].

There is another interesting method credited to Bessel [2]. Here the object and image planes are fixed. It is ascertained that the separation L between the two planes is equal to or greater than the focal length of the lens to be measured. This gives two positions of the lens where the image of the object is in focus as shown in Fig 12. The distance between these positions is taken as *d*. Then the focal length of the lens is given by

$$f = \frac{L^2 - d^2}{4L} \tag{49}$$

The method requires measurement of two distances only.

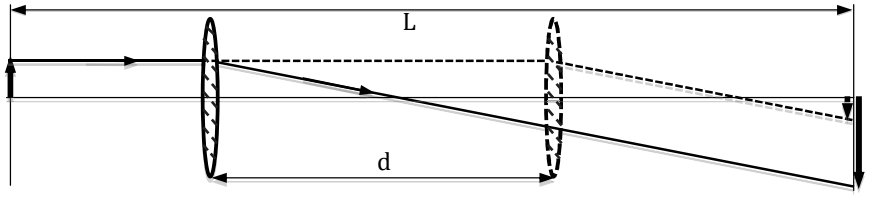

Fig 12. Bessel method to determine focal length of a positive lens

Recently a method has been described to measure focal length with high precision using imaging conjugates [20].

B-1.5 Focal length of a negative/diverging lens

The focal length of a diverging lens cannot be determined directly. There are other indirect methods to determine the focal length of a diverging lens. One of the methods, known as virtual object method requires a positive lens of a shorter focal length than that of the diverging lens. Figure [13] shows the schematic of image formation by a combination of positive and negative lenses. It may be noted that the lenses need not be in contact.

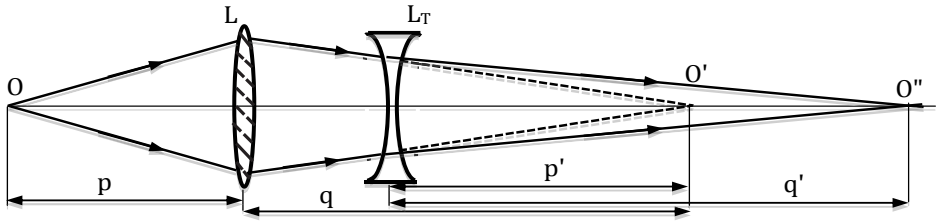

Fig 13. Determination of the focal length of a diverging lens

Positive lens L makes an image of a source at O at the image position O'. When the test lens L_T is inserted in the light path and properly positioned, the image shifts to O". The focal length is calculated from

$$f = \frac{p'q'}{p' - q'} \tag{50}$$

B-1.6 Nodal slide method

The method is based on the fact that the nodal planes and principal planes are coincident when the media on both sides of the lens are same and the rotation of the lens about the rear nodal point does not shift the image.

In practice, an object say a fine mesh is illuminated by a light source and imaged by a test lens, which is placed on a nodal slide. The lens is placed on a translation stage, which is mounted on a rotatable mount. The axis of rotation can be made to pass through any portion of the lens by moving the translation stage. This arrangement is called a nodal slide. The lens is so positioned that the axis of rotation passes through the nodal point. In such a situation, rotation of the lens does not shift the image. Indeed this criterion is used to locate the nodal plane. Since the nodal plane is coincident with the principal plane, the distance between the image plane and the axis of rotation is the focal length.

B-1.7 Focal length measurement from the difference between conjugate positions

Several methods described here assume the lens to be a thin lens, which is a mathematical idealization. A lens is bound by two surfaces and has a finite central thickness. The focal length is the distance between the respective principal plane and focal plane. Nodal slide method locates the nodal plane. A method is described which uses the data, which is the difference between the object positions and image positions [20]. However, to obtain these difference data, we need to find a reference with respect to which the measurements are made. Fortunately the second focal point can be found by placing the lens in a collimated beam and this point is taken as a reference with respect to which the measurements are made for different object positions. Figure [14] shows the various locations of the point object.

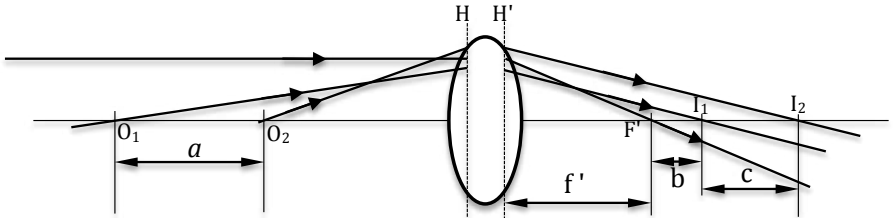

Fig 14. Imaging by a lens

When the point object is at infinity, its image is formed at the second focal point and the distance f' is the distance between the principal plane H' and the focal plane F'. The image of point object O_1 is

formed at I_1 and that of O_2 is formed at I_2. To receive the images, the screen/detector is to be moved by b and c, which are measured on the bench. Similarly the distance between O_1 and O_2 is measured on the optical bench and is equal to *a*. The focal length *f ′* is calculated from the measured values *a*, *b* and *c*. The formula is obtained by using the imaging conditions, that is

$$\frac{1}{p} + \frac{1}{f' + b} = \frac{1}{f'} \tag{51a}$$

and

$$\frac{1}{p - a} + \frac{1}{f' + c} = \frac{1}{f'} \tag{51b}$$

where *p* is the object distance for the point O_1 as measured from the principal plane H. Eliminating *p* and rearranging, we obtain

$$f' = \sqrt{\frac{abc}{(c - b)}} \tag{52}$$

Thus the focal length is obtained by using the measured difference values and hence the focal length is determined with higher accuracy.

B-1.8 Moiré deflectometry [*21, 22*]

Consider a situation where the lens is illuminated by a collimated beam, which is brought to focus by the test lens. In the convergent beam are placed two identical Ronchi gratings of pitch *p*. Let their separation be *Δ* as shown in the Fig 15. They are placed such that their rulings are parallel.

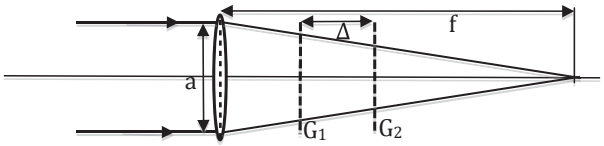

Fig 15. Moiré formation for focal length measurement

The grating G_1 is projected on grating G_2 and hence its pitch becomes smaller. If the illuminated size of the grating G_2 is *L* and that of G_1 is *L*+*y*, then the pitch p' is related to pitch p as

$$p' = \frac{L}{L + y}\, p \quad \Rightarrow \frac{p}{p'} = 1 + \frac{Y}{L} \tag{53}$$

The moiré fringes are formed due to pitch mismatch. The pitch *d* of the moiré fringes is $d = \frac{pp'}{p - p'}$ $= \frac{pL}{y}$. Further, from the Fig 15 we have $\frac{a}{f} = \frac{y}{\Delta}$. Substituting for *y*, we obtain

$$f = \frac{a\Delta}{pN} \tag{54}$$

where *N* (*L*/*d*) is number of fringes observed over the grating G_2 of size *L*. Therefore the focal length is determined by noting the number of moiré fringes observed with identical Ronchi gratings.

Conclusion and Acknowledgement

Curvature and focal length are basic parameters that need to be measured accurately during the production stage. A number of methods have been developed and reported in standard textbooks on Optics. It is not possible to acknowledge the contribution of each and every researcher. An attempt has been made to place these methods in a single paper with limited references. My colleagues at the Applied Optics Laboratory, Indian Institute of Technology Madras have been quite active in experimental optics and I would like to acknowledge their work and support. This article is dedicated to Prof. G D Baruh, formerly at Dibrugarh University, Assam, India, who is a great teacher.

References

1. Jenkins F A, White H E, *Fundamentals of Optics*, McGraw-Hill, New York, 1950.
2. Meyer-Arendt J R, *Introduction to Classical and Modern Optics*, Prentice-Hall, Hall, Englewood Cliffs, NJ, 1989.
3. Pedrotti F L, Pedrotti L S, *Introduction to Optics*, Prentice-Hall, Englewood Cliffs, NJ, 1987.
4. Begunov B N, Zakaznov N P, Kiryushin S I, Kuzichev V I, *Optical Instrumentation - Theory and Design*, MIR Publications, Moscow, 1988.
5. Malacara J Z, Angle, Distance, Curvature, and Focal Length Measurements, in Optical Shop Testing, (Ed D. Malacara), John Wiley and Sons, Inc., New York, 1992.
6. Malacara Daniel, Malacara Zacarias, *Optical Metrology*, Chapter 29, pp.29.1-29.31, in Handbook of Optics, Vol. II, (2nd edn), Editor-in-Chief Michael Bass, McGraw-Hill, Inc. New York, 1995.
7. Medicus Katherine Mary, Improving Measurements based on the Cat's eye Retro-reflection, Ph D Thesis, The University of North Carolina at Charlotte, 2006.
8. Selberg L, Radius measurement by interferometry, *Opt Engg*, 31(1992)1961-1966.
9. Irick S C, Franck A D, Radius of curvature limitation and accuracy of a surface profile measurement, Lawrence Berkley National Laboratory Note 604, July 2001.
10. Schmitz T L, Davies A D, Evans C J, Uncertainties in interferometric measurements of radius of curvature, in Optical Manufacturing and Testing IV, (Ed H P Stahl), *Proc SPIE*, 4451(2001)432-447.
11. Griesmann U, Soons J, Wang Q, DeBra D, Measuring Form and Radius of Spheres with Interferometry, *Annals of the CIRP, Manufacturing Technology*, 53(2004)451-454.
12. Sacramento-Solano J D, Granados-Agustın F S, Cornejo-Rodrıguez A A, Measurements of local radii of curvature by the retro-collimated interferometric method, *Revisita Mexicana De Fisica*, 54(2008)194-199.
13. Xiao Muzheng, Jujo Satomi, Takamasu Kiyoshi, Takahashi Satoru, Nanometer Profile Measurement of Large Aspheric Optical Surface by Scanning Deflectometry with Rotatable Devices, - Error Analysis and Experiments- Proceedings of the 11theuspen International Conference – Como – May 2011
14. Mejía-Barbosa Yobani, Malacara-Hernández Daniel, A Review of Methods for Measuring Corneal Topography, Optometry and Vision Science, Vol. 78, No. 4, April (2001)240-253.
15. Zhao Chunyu, Zehnder Rene, Burge James H, Measuring the radius of curvature of a spherical mirror with an interferometer and a laser tracker, *Opt Eng*, 44(2005) 090506-1.
16. Mantravadi M V, Malacara D, Newton, Fizeau, and Haidinger Interferometers, in Optical Shop Testing, (Edited by Daniel Malacara), John Wiley & Sons, Inc. 3rd edn, 2007
17. Gerchman Mark C, Hunter George C, Differential technique for accurately measuring the radius of curvature of long radius concave optical surfaces, *Proc SPIE,* 192(1979)75-84.
18. Su Tianquan, Park Won Hyun, Parks Robert E, Su Peng, Burge James H, Scanning Long-wave Optical Test System – a new ground optical surface slope test system, Optical Manufacturing and Testing IX, (Edited by James H. Burge, Oliver W. Fähnle, Ray Williamson), *Proc SPIE,* 8126(2011)81260E1-10.
19. Malacara-Doblado Daniel, Measuring the curvature of spherical wavefronts with Talbot interferometry, *Opt Eng*, 36(1997)2016-2024.
20. Liao Lin-Yao, Bráulio de Albuquerque F C, Parks Robert E, Sasian José M., Precision focal-length measurement using imaging conjugates, *Opt Engg*, 51(2012)113604
21. Changlun Hou, Jian Bai, Xiyun Hou, Chen Sun, Guoguang Yang, Novel method for testing the long focal length lens of large aperture, *Optics and Lasers in Engg*, 43(2005)1107-1117.
22. Trivedi Satyaprakash, Dhanotia Jitendra, Prakash Shashi, Measurement of focal length using phase shifted moire´ Deflectometry, *Optics and Lasers in Engg*, 51(2013)776-782.

[*Received*: 27.10.2014; *accepted*: 1.11.2014]